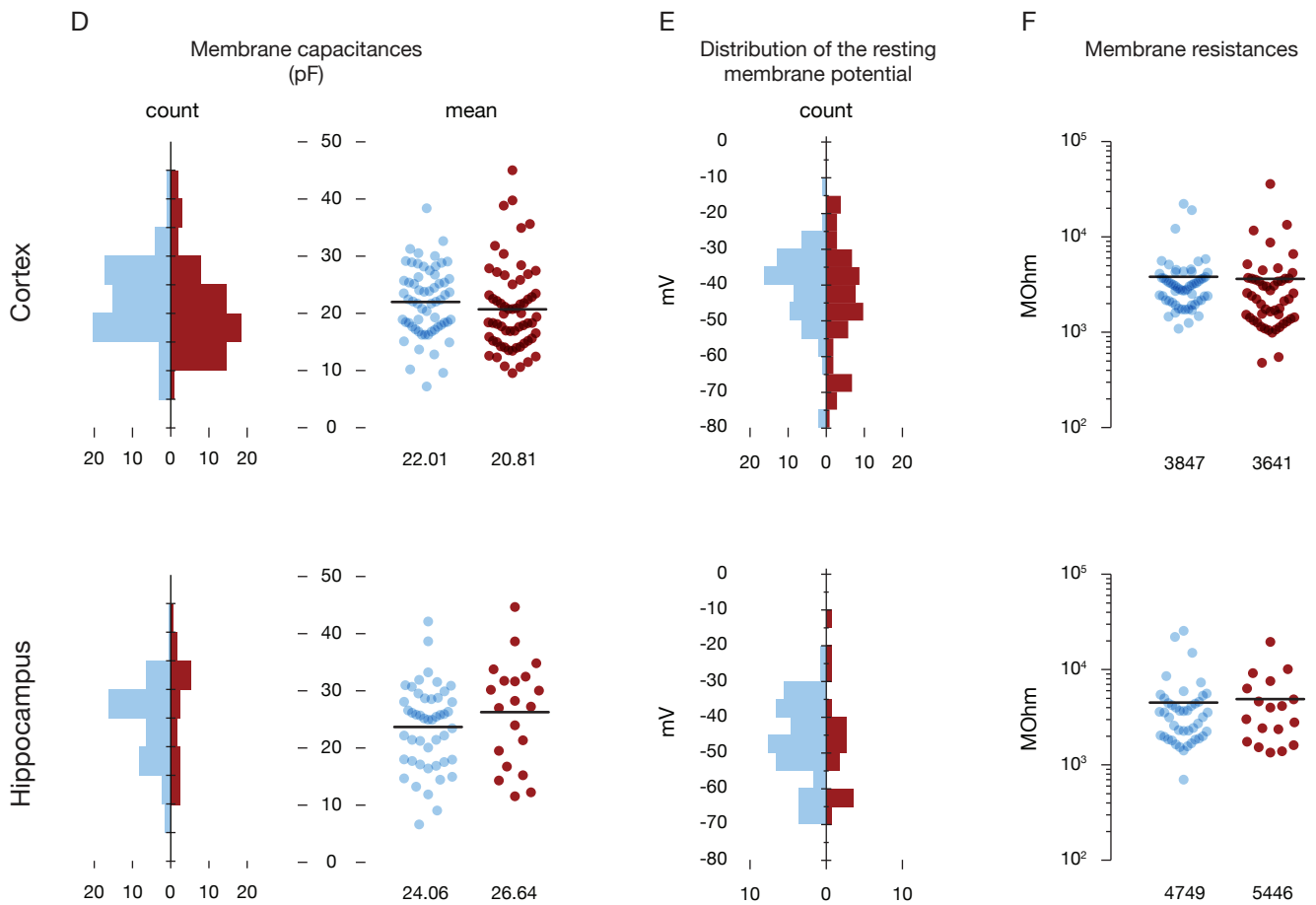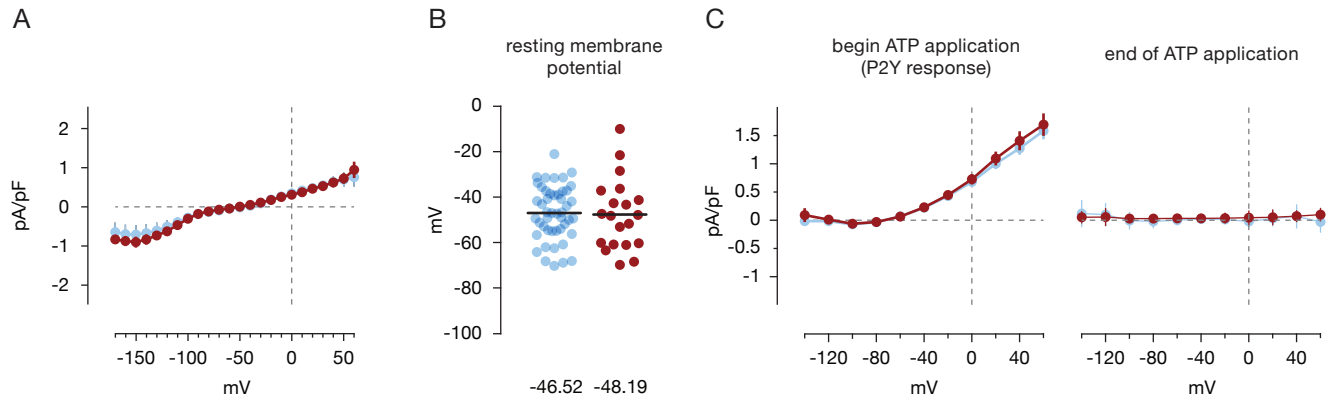**Supplemental Information**

Transcriptional and Translational Differences

# of Microglia from Male and Female Brains

Dilansu Guneykaya, Andranik Ivanov, Daniel Perez Hernandez, Verena Haage, Bartosz Wojtas, Niklas Meyer, Meron Maricos, Philipp Jordan, Alice Buonfiglioli, Bartlomiej Gielniewski, Natalia Ochocka, Cagla Cömert, Corinna Friedrich, Lorena Suarez Artiles, Bozena Kaminska, Philipp Mertins, Dieter Beule, Helmut Kettenmann, and Susanne A. Wolf

A

B

resting membrane potential

-46.52 -48.19

C

begin ATP application
(P2Y response)

end of ATP application

D

Membrane capacitances
(pF)

count

mean

Cortex

20 10 0 10 20

22.01 20.81

Hippocampus

20 10 0 10 20

24.06 26.64

E

Distribution of the resting
membrane potential

count

20 10 0 10 20

10 0 10

F

Membrane resistances

3847 3641

4749 5446

Legend: ● male   ● female

Supplemental Figure 1. Passive membrane properties of patched microglia, Related to Figure 2

Membrane currents were recorded from microglia located in acute hippocampal and cortical slices while clamping the cell to -70 mV as described in figure 2. (A) The average current density (pA/pF) to voltage (mV) relationship was obtained from hippocampal microglia. Microglia derived from male mice show no significant difference in baseline inward and outward conductances compared to female. (B) Distribution of reversal potentials from male and female microglia. Microglial cells derived from female mice showed no significant difference in the resting membrane potentials compared to male. Average values indicated at the bottom. (C) To construct the current density to voltage relationship (pA/pF to mV) of the ATP-activated current component, values before ATP application were subtracted from currents at the peak of the response of the induced inward current and the peak of the induced outward current as indicated in figure 2. No significant differences in the reversal potential as well as in the inward or outward conductance upon ATP application were observed between sexes. 3 animals per group were used, and the number of recorded hippocampal microglia was for males n = 19 and for females n = 15. (D) Summary of the membrane capacitance represented as scatter plots and histograms reveals no significant differences between male and female both in hippocampus and cortex. (E) Distribution of the reversal potentials shown as averaged histograms of microglia from male and female animals. (F) Scatter plot depicting the membrane resistances shows no significant differences between male and female in both regions.
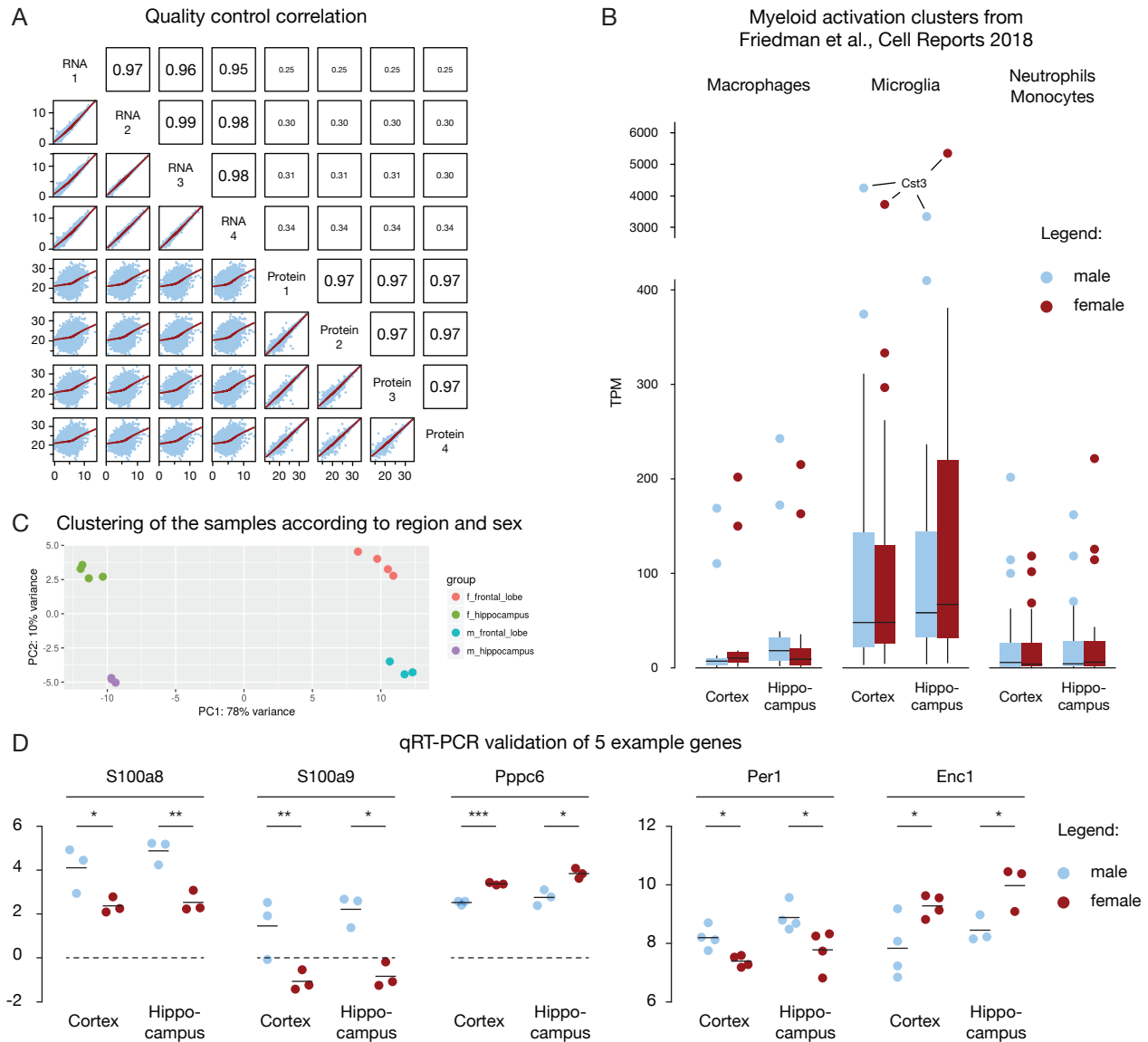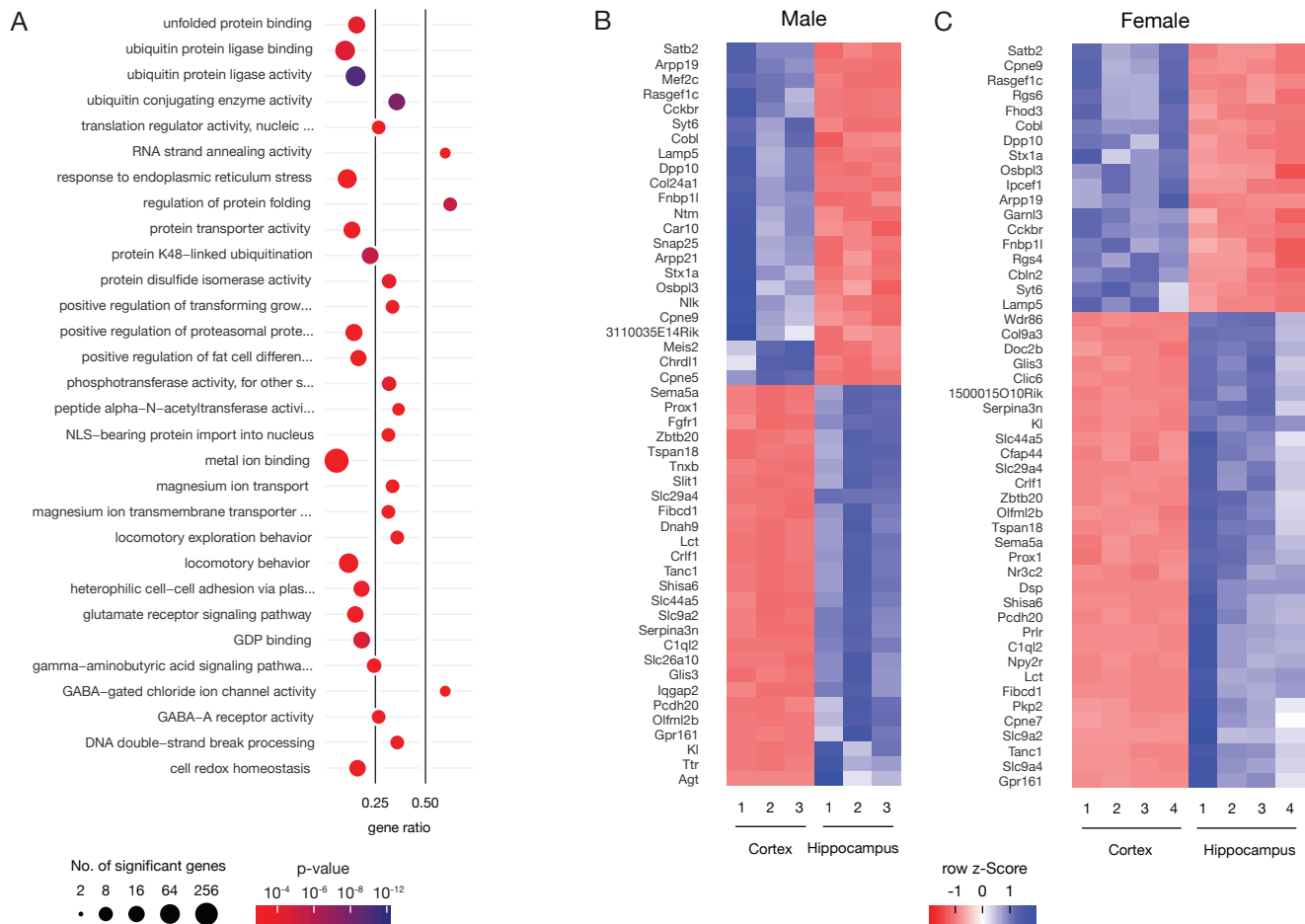
Supplemental Figure 2. Sex dependent transcriptome profile, Related to Figure 4
(A) Cross-comparison of RNA (from hippocampus) and protein (total brain) expression levels: The X and Y axes of the scatter plots represent the gene log2 TPMs or log2 iBAQ intensity in each sample. Red lines are the running averages. Pearson's correlation coefficients for each of the comparisons are depicted in the upper panels of the diagonal. The correlation is the highest within RNA replicates and within protein replicates, whereas correlation between proteins and RNA is low. (B) Friedman et al., (Cell Reports 2018) identified co-regulated gene modules from transcriptional profiles of CNS myeloid cells in different mouse models. The analysis incorporated RNA sequencing data from more than 300 expression profiles across different brain disease models, developmental stages, brain regions and myeloid cell types. In particular, clustering of normalized gene expression values identified microglia, macrophage and neutrophil/monocyte gene modules. To check for possible contamination in our sequencing data we compared the gene expression values in these modules. Box plots show the distribution of gene expression in different myeloid activation modules. Y-axis is TPM: (transcript per million). Supplementary table 1 contains genes in each three modules. (C) Principal component analysis of RNA-Seq samples. (D) qRT-PCR in freshly isolated microglia from hippocampus and cortex. Delta Ct values of 5 selected differentially expressed genes between male and female samples. Data are shown as the delta ct compared with endogenous TBP as mean ± s.e.m. At least 3 mice per n and three n per group were analyzed. Significant differences were analyzed by an unpaired Student t test (*P < 0.05, **P < 0.01, ***P < 0.001).

Supplemental Figure 3. Sex dependent transcriptome profile, Related to Figure 5
(A) Gene ontology analysis of hippocampus female: top 15 molecular functions and top 15 biological processes. (B-C) Heat maps show the top 50 (sorted by adj. p-value) differentially regulated genes for each of the comparisons in hippocampus vs. cortex in male and female samples. Z-scores are calculated per gene from TPM (transcript per million) values of each replicate.
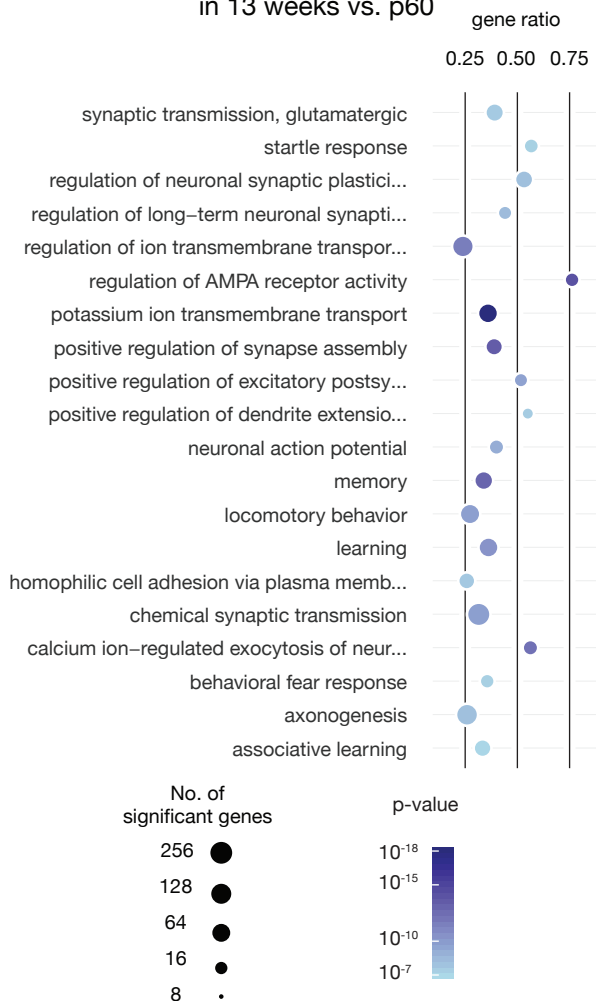
A

Correlation of log2 fold changes of p60 and 13 weeks
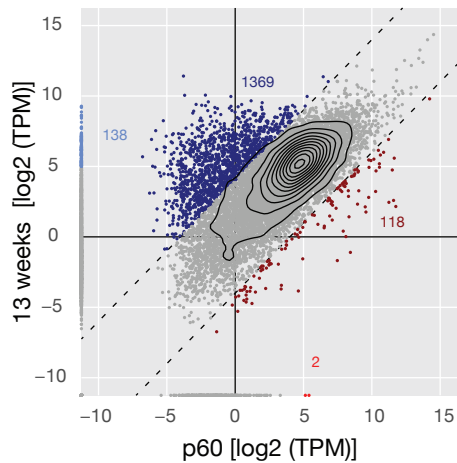
B

CDS length
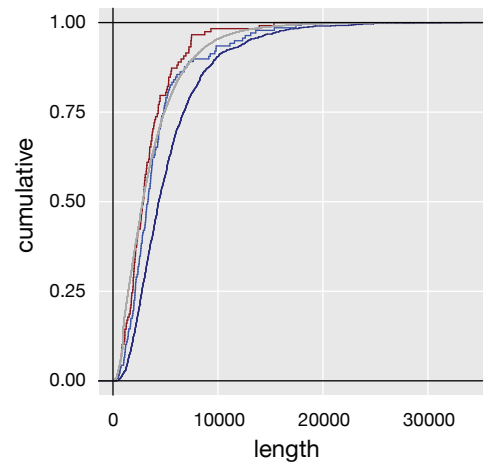
C

GO enrichment analysis of higher expressed genes in 13 weeks vs. p60


Supplemental Figure 4. Comparison of male hippocampal transcriptome profile at 13 weeks with P60 data set (Hanamsagar et al. 2017), Related to Figure 4

(A) Figure shows the comparison of the mean (over replicates) gene TPM values between our RNA-Seq (male hip-pocampus, 13-week-old mice) samples and RNA-Seq samples from Hanamsagar et al. study (male hippocampus, P60). Hanamsagar et al. measured the expression levels of total RNA: SRR5642497, SRR5642498, SRR5642499, SRR5642500 (in total ~14 million single ended reads, with 86-92% unique mappability). We sequenced polyA se-lected RNA, with 3 replicates (in total ~56 million paired end reads, with 93-94% unique fragment mappability). We detected 1369 genes (dark blue) with 16-fold higher TPMs in our data, while in Hanamsagar et al., only 118 (dark red). We also detected 138 highly expressed genes ($log2\_TPM > 5$, blue) in our data that had zero read counts in P60. In P60 study, only two genes were highly expressed ($log2\_TPM > 5$, red) and had no read counts in our study. (B) Comparison of the mRNA length between different groups of genes from the upper scatter plot. (C) Gene On-tology analysis of the blue and dark blue subpopulation of genes from the upper scatter plot. X-axis is the ratio between significantly differentially regulated genes and the total number of genes in that GO category. The X-axis and the size of the plots are analogous to Figure 5.
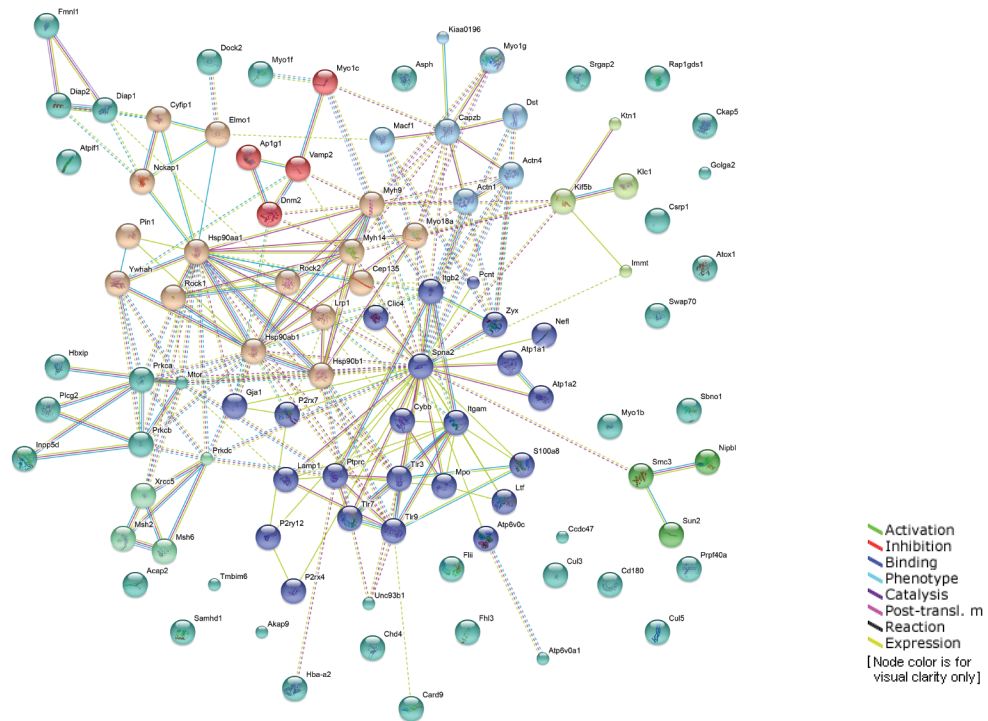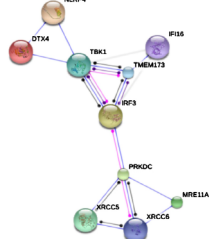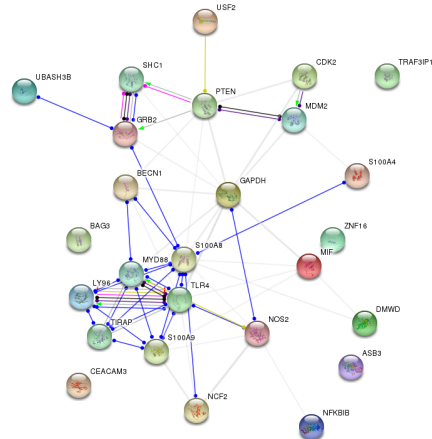
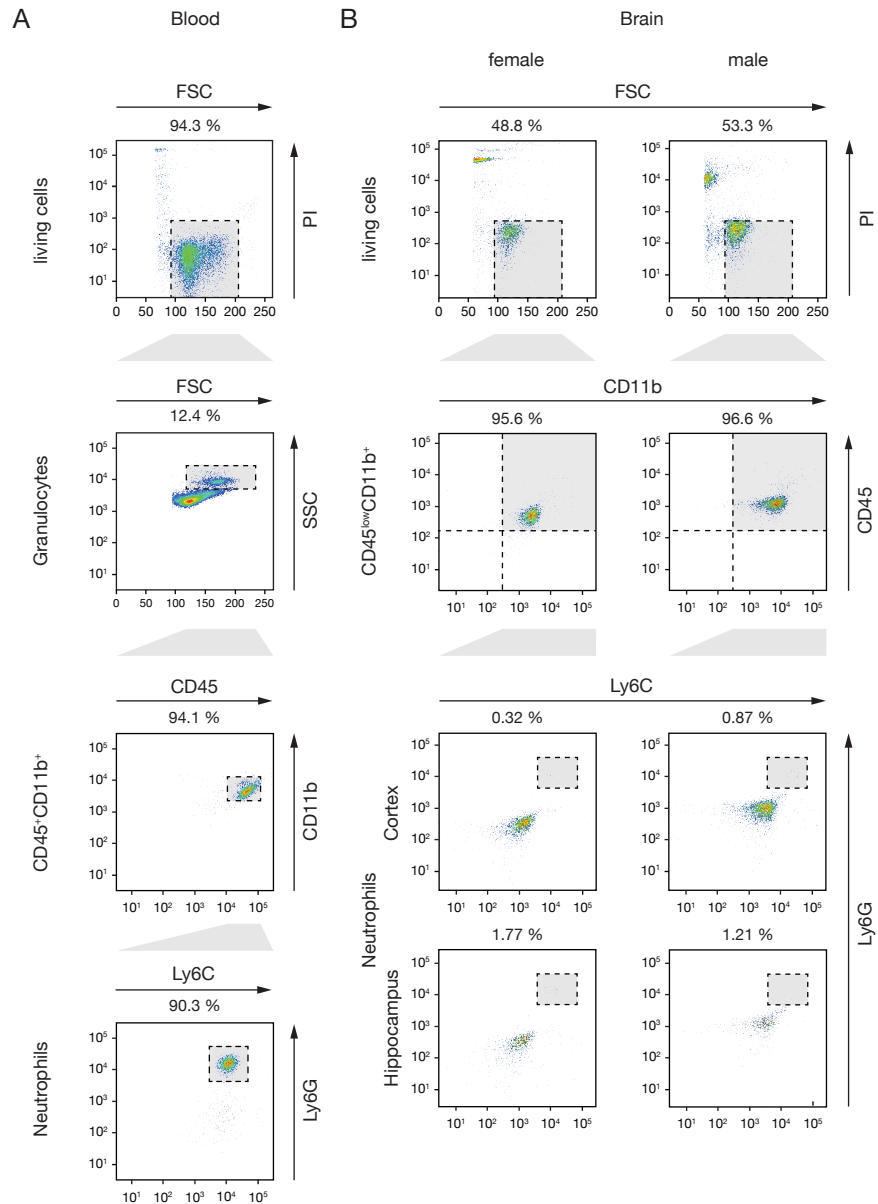**Supplemental Figure 5. Pathway analysis for proteins expressed at significantly higher levels in male microglia, Related to Figure 6**

Search Tool for the Retrieval of Interacting Genes/Proteins (STRING) pathway analysis of proteins. (A) Network of all proteins expressed at significantly higher level in male microglia from Mass spectrometry analysis. Each color represents different clusters (k-means clustering). The settings for the relationship between those proteins are the evidence as network meaning, and found in experiments or databases as active interaction sources. (B-C) STRING pathway analysis of specifically picked proteins that are involved in microglia regulation. Each color represents a different pathway related to microglia. Individual proteins are labeled by gene name, and thicker lines represent more evidence of association. (B) Irf3 related pathway: Irf3 was one of the few genes expressed higher level in the proteomic female data set. However, Prkdc and Xrccr5 were expressed at higher level in the male microglia proteo-me. (C) S1008a related pathway. This was one of the few genes expressed at higher level in the male data set from proteomic and transcriptomic analysis.

Supplemental Figure 6. Purity of CD11b+ cell population, Related to Figure 4 and 5
We show here a representative flow cytometry analysis of CD11b+ MACS sorted cells for the purity of the CD11b+ cell population. Blood samples were used to define the position of Ly6G+ neutrophil population in the gating strate-gy. CD11b+ cells were further defined in sub-populations using the expression of Ly6G (neutrophils) and Ly6C (monocytes). Less than 2% of the CD11b+ cell population are Ly6G positive in both male and female hippocampus and cortex.